JBC Papers in Press. Published on May 27, 2015 as Manuscript M114.612903
The latest version is at http://www.jbc.org/cgi/doi/10.1074/jbc.M114.612903

TPX2 inhibits Eg5 by interactions with both motor and microtubule

Sai K. Balchand[1], Barbara J. Mann[1], Janel Titus[1], Jennifer L. Ross[1,3] and Patricia Wadsworth[1,2]
Departments of Biology[2] and Physics[3] and Program in Molecular and Cellular Biology[1]
University of Massachusetts Amherst

Correspondence:
P. Wadsworth
University of Massachusetts Amherst
Biology Department, 221 Morrill South
611 North Pleasant St, Amherst, MA 01003

Running title: TPX2 inhibition of Eg5

Abbreviations: EGFP, enhanced green fluorescent protein

Key words: kinesin, microtubule-associated protein (MAP), microtubule, mitosis

Background: TPX2 is a mitotic microtubule-associated protein that regulates the kinesin, Eg5.
Results: Full-length TPX2 is a more potent inhibitor of Eg5 velocity than truncated TPX2; differential regulation by TPX2 was not observed for monomeric Eg5.
Conclusion: TPX2 inhibits Eg5 as a roadblock and by direct interaction with Eg5.
Significance: TPX2 may contribute to the spatial and temporal regulation of the mitotic motor Eg5.

ABSTRACT

The microtubule-associated protein, TPX2, regulates the activity of the mitotic kinesin, Eg5, but the mechanism of regulation is not established. Using total internal reflection fluorescence (TIRF) microscopy, we observed that Eg5, in extracts of mammalian cells expressing Eg5-EGFP, moved processively toward the microtubule plus-end at an average velocity of 14 nm/s. TPX2 bound to microtubules with an apparent dissociation constant of ~ 200 nM and microtubule binding was not dependent on the C-terminal tails of tubulin. Using single molecule assays, we found that full-length TPX2 dramatically reduced Eg5 velocity whereas truncated TPX2, which lacks the domain that is required for the interaction with Eg5, was a less effective inhibitor at the same concentration. To determine the region(s) of Eg5 that are required for interaction with TPX2, we performed microtubule-gliding assays. Dimeric, but not monomeric, Eg5 was differentially inhibited by full-length and truncated TPX2, demonstrating that dimerization, or residues in the neck region, are important for the interaction of TPX2 with Eg5. These results show that both microtubule binding and interaction with Eg5 contribute to motor inhibition by TPX2 and demonstrate the utility of mammalian cell extracts for biophysical assays.

Introduction

Accurate chromosome segregation during cell division requires the assembly and function of the mitotic spindle. The spindle is composed of a bipolar array of dynamic microtubules that are required for chromosome alignment and segregation. Mitotic motor proteins play important roles in regulating microtubule organization and dynamics and in generating the forces required for spindle formation and chromosome motion. Despite the characterization of many mitotic motor proteins, how their activity is regulated both spatially and temporally in the spindle remains incompletely understood (1).

TPX2 is a conserved mitotic microtubule-associated protein (MAP) that was originally identified as a protein required for the dynein-dependent targeting of the *Xenopus* kinesin Xklp2 to mitotic spindle poles (2). In mammalian cells, TPX2 localizes to the nucleus in interphase and to the spindle in mitosis with an enrichment near spindle poles (3,4). Depletion of TPX2 using siRNA results in short bipolar or multipolar spindles that fail to progress through mitosis (3,4). The N-terminus of TPX2 binds and activates the mitotic kinase Aurora A, and is required to localize the kinase to spindle microtubules (5-7). During spindle formation, TPX2 is required for microtubule formation near kinetochores, an activity that requires GTP bound Ran which relieves the inhibitory action of importin α/β on TPX2 (8). In addition, it has been demonstrated that the C-terminus of TPX2 binds to the bipolar kinesin Eg5 and targets the motor to spindle microtubules (9,10). Expression of TPX2 lacking the C-terminal 35 amino acids, which contribute to Eg5 binding, results in defective spindles with greatly reduced Eg5 on spindle microtubules, unfocussed spindle poles and bent and buckled microtubules (11).

Because Eg5 plays a critical and conserved function in establishing spindle bipolarity, it is important to understand how this motor is regulated in the spindle. Previous *in vitro* experiments have shown that purified TPX2 reduces the velocity of Eg5-dependent microtubule gliding and microtubule-microtubule dependent sliding (11). Eg5 accumulation on microtubules is enhanced in the presence of full length TPX2, but less in the presence of TPX2 lacking the Eg5 binding domain (11). These results directly demonstrate that TPX2 inhibits the ability of Eg5 to translocate microtubules, but the mechanism of inhibition is not established. Here we use *in vitro* assays and single molecule TIRF microscopy to characterize the interaction of TPX2 with microtubules and to examine the behavior of Eg5 in the presence of TPX2. Our results demonstrate that TPX2 blocks Eg5 motility by both a direct interaction with Eg5 and by binding to microtubules and acting as a roadblock. Using microtubule

gliding assays, we further show that dimeric, but not monomeric, Eg5 is differentially inhibited by full-length and truncated TPX2. Our experiments provide new insight into the microtubule-associated protein TPX2 and its regulation of the mitotic kinesin Eg5.

Materials and Methods

Materials

All chemicals, unless otherwise specified, were purchased from Sigma-Aldrich.

Cell culture

LLC-Pk1 cells were cultured in a 1:1 mixture of F10 Hams and Opti-MEM (Life Technologies, Grand Island, N.Y.) containing 7.5% fetal bovine serum and antibiotics at 1X and 5% CO_2. Cell extracts were made from LLC-Pk1 cells stably expressing LAP-tagged Eg5 from a bacterial artificial chromosome (12). To prepare the extract, a confluent 100 mm diameter cell culture dish was washed twice with 5 ml of room temperature PBS. Then, 300 µl of extraction buffer containing 40 mM HEPES/KOH pH 7.6, 100 mM NaCl, 1 mM EDTA, 1 mM PMSF, 10 µg/ml Leupeptin, 1 mg/ml pepstatin, 0.5% Triton X 100 and 1 mM ATP (13) was added dropwise to the dish and incubated for approximately 2 min, without disrupting the monolayer. The cell extract was transferred to a microcentrifuge tube and centrifuged at 14,500 RPM at 4°C for 10 min in a tabletop centrifuge. The supernatant was recovered and aliquoted into small tubes, flash frozen and stored in liquid nitrogen. Protein concentration was determined using the method of Lowry (14). For fluorescent intensity measurement experiments with Eg5-mEmerald, an siRNA resistant Eg5-mEmerald construct was transiently co-transfected into LLC-Pk1 cells with siRNA directed against endogenous Eg5 (target sequence CUGAAGACCUGAAGACAAU). The extract was made 48 hours post transfection as described. For the extracts used in size exclusion chromatography, siRNA treatment against endogenous Eg5 was omitted.

Construction of plasmids

For bacterial expression, desired nucleotide sequences of human TPX2 constructs (full length or truncated at amino acid 710) were cloned into a pGEX vector following an N-terminal GST tag and a ULP1 protease cleavage site (15). At the C-terminus of TPX2, the stop codon was removed and the Halo tag sequence was introduced. Constructs were verified by sequencing. For expression in SF9 insect cells, nucleotides coding for full length or the first 710 amino acids of human TPX2 were cloned into the pFast Bac A vector after an N terminal 6X His tag and the constructs were verified by sequencing. The virus for infecting the cells was obtained following the Bac-to-Bac protocol (Invitrogen, Grand Island, NY). The plasmid for monomeric Eg5-367 containing the first 367 amino acids of human Eg5 was a kind gift from the laboratory of Dr. Sarah Rice. The plasmid for the expression of dimeric Eg5-513 containing the first 513 amino acids of Eg5 was the kind gift from the laboratory of Dr. Susan Gilbert.

Protein purification

Full length TPX2 and TPX2-710 were expressed and purified from Sf9 cells using the Bac-to-Bac expression system (Invitrogen, Grand Island, NY). Infected cells were harvested, washed with ice-cold water and resuspended in lysis buffer (50 mM potassium phosphate pH 8, 250 mM KCl, 40 mM imidazole, 1% NP-40, 10 mM beta mercaptoethanol, and a protease inhibitor tablet (Roche, Indianapolis, IN) on ice. The lysate was spun at 125,000 x g for 45 min at 4°C. The supernatant was loaded onto pre-equilibrated Ni NTA agarose beads (Qiagen, Valencia, CA) and incubated for 90 min at 4°C with end-over-end shaking. The flow through was removed and beads were washed with wash buffer (same as lysis buffer with 10% glycerol and 0.01% NP-40). The protein was eluted with elution buffer (50 mM potassium phosphate pH 7, 150 mM KCl, 250 mM imidazole, 10% Glycerol, 10 mM beta mercaptoethanol, and 0.01% NP-40) and dialyzed in a buffer containing 25 mM HEPES, pH 7.6, 10 mM KCl, 2 mM MgCl2, 10% Glycerol, 0.01% NP-40 and 1 mM DTT for 4 hours at 4°C. Aliquots were flash frozen in liquid nitrogen and stored at -80°C.

Full length TPX2-Halo and TPX2-710-Halo were expressed and purified from *E.coli* Rosetta DE3 pLysS cells. In short, 500 ml of culture was grown to an optical density of 0.5-0.8, induced with 0.1 mM IPTG at 18°C for 16 hours. The bacteria were harvested and washed with ice-cold distilled water. The cell pellet was resuspended in 2X lysis buffer (60 mM HEPES pH 7.4, 0.4 mM EGTA, 2 mM DTT, 1.4 µg/ml pepstatin, 1.0 mM Pefabloc, 4 µg/ml leupeptin, and 2 µg/ml Aprotinin), diluted to 1X with cold dH_2O, sonicated on ice (3X 30 s at maximum setting), and clarified at 15,000 x g for 20 min at 4°C. The supernatant was incubated for 1 hour at 4°C with Glutathione sepharose beads that were pre-equilibrated in lysis buffer. The beads were then washed 3X in wash buffer (10% glycerol, 300 mM KCl, 0.1% Triton X-100, 1 mM DTT, 0.7 µg/ml pepstatin and 0.5 mM Pefabloc) and twice in TEV buffer (5 mM Tris pH 8.0, 150 mM KCl, 10% glycerol, 0.1% Triton X-100, 1 mM DTT and 0.5 mM Pefabloc). The beads were resuspended in TEV buffer and incubated with 23 µM Halo tag Alexa fluor 660 (Promega, Madison, WI) for 15-20 min at room temperature and then washed to remove unbound ligand. The beads were then resuspended in TEV buffer containing Ulp1 protease and incubated at 16°C for 1 hr to cleave protein off the beads. The supernatant containing the protein was collected by centrifugation and aliquots were flash frozen and stored in liquid nitrogen.

Monomeric Eg5-367 was purified from *E.coli* as described in (16). Briefly, 500 ml of bacteria was grown and induced at an OD of 0.5-0.8 with 0.1 mM IPTG and incubated at

16°C for 16 hours. The bacteria were pelleted and washed with ice-cold water. The pellet was resuspended in lysis buffer (10 mM sodium phosphate buffer pH 7.2, 20 mM NaCl, 2 mM $MgCl_2$, 1 mM EGTA, 1 mM DTT, and 0.1 mM ATP with protease inhibitor tablet) and lysed by sonication. The lysate was clarified by centrifuging at 15,000 x g for 30 min at 4°C. The supernatant was incubated with pre-equilibrated Ni NTA agarose beads for 90 min at 4°C. The beads were then washed in wash buffer (same as lysis buffer containing 20 mM imidazole) and eluted in elution buffer (same as lysis buffer with 300 mM imidazole). The eluate was then dialyzed against buffer containing 20 mM HEPES pH 7.2, 5 mM magnesium acetate, 0.1 mM EDTA, 0.1mM EGTA, 50 mM potassium acetate, 1 mM DTT, and 5% sucrose for 4 hours at 4°C. Aliquots were flash frozen in liquid nitrogen and stored at -80°C. Dimeric Eg5-513 was expressed and purified from *E.coli* exactly as described (11).

TPX2 co-sedimentation with microtubules

Unlabeled tubulin prepared from porcine brains (17) was polymerized and resuspended in PEM 100 buffer containing 50 µM Taxol. 500 nM full length TPX2 or TPX2-710 was incubated with indicated concentration of unlabeled polymerized microtubules at room temperature for 10 min. The mixture was centrifuged for 10 min at room temperature in a tabletop centrifuge at maximum speed. The supernatant and pellet fractions were carefully separated. Samples for SDS electrophoresis were prepared by boiling the samples with SDS protein sample buffer and run on an 8% polyacrylamide gel. The proteins were then transferred to a PVDF membrane and probed using antibodies against TPX2 (Novus Biologicals, Littleton, CO) and tubulin (DM1A, Sigma-Aldrich). The blots were developed by chemiluminescence and captured on a Biorad (Hercules, CA) imaging station. Analysis of band intensities were performed using ImageJ. Data were plotted using KaleidaGraph and fit with a quadratic equation (15). Subtilisin A treated microtubules were prepared as described (15).

TPX2-Halo Microtubule Binding Assays

For TPX2-Halo binding experiments, first 10 µL of 10% Rat YL ½ (0.1 mg/ml) anti-tubulin antibody (Accurate Chemical, Westbury, N.Y.) was added to the flow chamber and incubated for 2 min. Second, 0.1 mg/ml Rhodamine-microtubules (untreated or treated with Subtilisin A) were flowed in and incubated for 2 min. Third, the surface was blocked by adding 5 % Pluronic F-127 and incubated for 2 min. For assays done in epifluorescence, the chamber was incubated with the indicated concentration of TPX2-Halo for 2 min in PEM 100, [100 mM K-Pipes, pH 6.8, 2 mM MgSO4, and 2 mM EGTA] plus 0.5% Pluronic F-127, 50 µM

taxol, 5 mM DTT, 15 mg/ml glucose, 1.23 mg/ml glucose oxidase and 0.375 mg/ml catalase). Salt (KCl) from a 10 X stock of the working concentration was added directly to the buffer. Wide field images were acquired with a constant exposure time. To measure dwell times of TPX2-Halo and TPX2-710-Halo, experiments were performed using TIRF microscopy.

Eg5 single molecule experiments

The concentrations of Eg5 in the extracts were measured by quantitative Western blots. For the single molecule experiments, the perfusion chambers were made from glass slides, silanized coverslips and double stick tape. 10 µL of 10% Rat YL ½ anti-tubulin antibody (Accurate Chemical, Westbury, N.Y.) was flowed into the chamber and incubated for 3 min. Then, the chamber was blocked by flowing in 5% Pluronic F127 for 3 min. Diluted Cy5 labeled microtubules (composed of a mixture of Cy5 tubulin (Cytoskeleton, Inc, Denver, CO) and unlabeled brain tubulin) were flowed into the chamber and incubated for 3 min followed by a second block of 5% pluronic F127. Eg5 was diluted to 1 or 1.5 nM in motility buffer containing PEM 50 (50 mM Pipes pH 6.9, 2 mM EGTA, 2 mM MgSO4), 0.5% F127, 5 mM ATP, 1 mM DTT, 25 µM Taxol supplemented with oxygen scavenging system (15 mg/ml glucose, 1.23 mg/ml glucose oxidase and 0.375 mg/ml catalase) and flowed into the chamber and imaged. For pre-incubation experiments with TPX2, the indicated concentrations of TPX2 were added to the motility buffer along with Eg5 in extract and incubated on ice for 2 min before flowing into the chamber.

Kinesin-1 single molecule experiments

Perfusion chambers were made as described above. 10 µL of 10% Rat YL ½ anti-tubulin antibody, 5% pluronic F127, and diluted Cy5 labeled microtubules were added sequentially and incubated for 5 min each. The chamber was washed with PEM 100 plus Taxol. Kinesin-1 was diluted in PEM 100 with 10 mM DTT. This was then added to the motility buffer (PEM100, 25 µM Taxol, 0.5% F127, 0.5 mg/mL BSA, oxygen scavenging system, and 0.5 mM ATP) and flowed into the chamber and imaged. For experiments with TPX2 addition, TPX2-Halo was diluted into the motility buffer (without Kinesin-1) and flowed into the chamber during image acquisition.

Microtubule-microtubule gliding assays

Biotinylated, Cy5 labelled microtubules were immobilized on silanized coverslips using anti-Biotin antibody (Sigma-Aldrich). The chamber was blocked using 5% F127. Eg5-EGFP from extracts was preincubated with rhodamine labelled microtubules for 3 min and the mixture was flowed into the

chamber. Finally, motility buffer was added followed by acquisition on a TIRF microscope.

Size Exclusion Chromatography

Eg5-EGFP was purified from SF9 insect cells as per manufacturer's instructions (Bac to Bac, Invitrogen, Grand Island, NY). The extract from LLC-Pk1 cells was prepared as mentioned before. The Superose 6 10/300 GL column (GE Healthcare, Pittsburgh, PA) was pre equilibrated with 10mM HEPES, pH7.6, 0.05% triton X100, 100mM NaCl, 1mM ATP before use. 100µL of the purified protein was loaded onto the column and run at a constant flow rate of 0.2ml/min. The Elution profile of Eg5-EGFP was directly followed by measuring absorbance at 488nm. For the size exclusion of LLC-Pk1 cell extracts, 175µL of cell extract was loaded on the column and run under identical conditions. The collected fractions were separated by SDS PAGE, transferred to a PVDF membrane and were probed for the presence of Eg5 using western blot.

Microtubule surface gliding assays

Perfusion chambers of approximately 10 µL volume were made using glass slides and coverslips with a double stick tape spacer. For gliding assays with the Eg5-367 monomer, the chamber was incubated with anti-His antibody and 2 mg/ml BSA for 3 min followed by two washes with motility buffer (80 mM PIPES pH 6.8, 2 mM MgCl2, 1 mM EGTA, 0.2 mg/ml BSA, and 150 mM sucrose). Then, the chamber was incubated with Eg5-367 for 3 min and washed again with motility buffer. Finally, the activation mix, consisting of motility buffer containing oxygen scavenging system, ATP, Taxol and diluted Cy5 labeled microtubules was added and imaged on a Nikon TiE microscope using epifluorescence. Surface gliding experiments with the dimeric Eg5-513 were performed exactly as described in Ma et al (2011). For TPX2 addition experiments, the TPX2 constructs were added to the activation mix, incubated for 2 min on ice and the flowed into the chamber.

Microscope Imaging and Analysis

TIRF microscopy was performed using a microscope (Ti-E; Nikon Instruments, Melville, N.Y.) equipped with a 60X 1.4 NA objective lens. The system was run by Elements software (Nikon Instruments, Melville, N.Y.). Images were acquired using a 512 x 512–pixel camera (Cascade II; Photometrics, Tuscon, AZ). A 4X image expansion telescope in front of the camera was used. The micron-to-pixel ratio was 68.5 nm/px. A blue diode laser (488 nm, 50 mW) was used. Images were acquired every 2 or 3 seconds for 10 min. For two color TIRF, a 488 nm argon laser and a 647 nm diode laser were used on a custom built TIRF system on a Nikon TiE stand, run by Elements software. A 60X objective lens was used; exposure times for both red and green illumination were

50-100 ms. Wide field Imaging for Eg5-513 gliding assays, and for binding of TPX2-Halo to microtubules, was performed using epifluorescence illumination.

Quantification of gliding velocity, single molecule velocity and MSD

The velocity of Eg5-513- and Eg5-367-dependent microtubule gliding movement was calculated using the MTrackJ plugin in ImageJ. To calculate the velocity of Eg5-EGFP single molecules from TIRF images, ImageJ was used to generate a kymograph of moving molecules. Velocities were calculated by manually tracking individual puncta. The data were ported to excel and a polynomial 2 trendline was added to the MSD vs time plot to determine D.

Results

TPX2 binding to microtubules

To examine the regulation of mammalian Eg5 by TPX2, we expressed and purified full-length TPX2 and a truncated version lacking the C-terminal 35 amino acids (referred to as TPX2-710) that mediate the interaction with Eg5 (10,11) (Fig. 1A). To characterize the microtubule binding of these proteins, we performed microtubule co-sedimentation experiments. Both full-length TPX2 and TPX2-710 co-sedimented with microtubules with apparent dissociation constants of 125 and 240 nM, respectively (Fig. 1B,C). Both full length and truncated TPX2 could be released from the microtubule lattice by adding KCl to the buffer, with negligible binding at 250 mM KCl. This demonstrates that, like other microtubule-associated proteins, TPX2 makes ionic interactions with the microtubule lattice (Fig. 2A).

Microtubule-associated proteins are thought to make electrostatic interactions specifically with the negatively-charged C-terminal E-hooks of tubulin, named for the abundance of glutamic acid residues (18). To determine whether the E-hooks are either a requirement for or facilitate TPX2 binding to microtubules, polymerized microtubules were digested with the enzyme Subtilisin A to cleave off the E-hooks and binding of TPX2 and TPX2-710 to control and digested microtubules was measured. The results show that binding of full length or truncated TPX2 to microtubules was not different for untreated, compared to Subtilisin digested, microtubules (Fig. 2B).

To examine the interaction of individual molecules of TPX2 with the microtubule we performed single molecule TIRF microscopy of Halo-tagged TPX2 full length and TPX2-710. Individual molecules were stationary on the microtubule lattice and, at the concentration examined, no enrichment at either end of the microtubule was observed.

The average dwell time of full length TPX2-Halo, measured from image sequences acquired at 2 s intervals for 15 min, was 60.1 sec (Fig. 2C). The average dwell time of Halo tagged TPX2-710 was 46.6 sec and was not statistically different from the Halo tagged full length TPX2.

Together these results demonstrate that TPX2 binds to the microtubule lattice with high affinity, and that the C-terminal 35 amino acids do not contribute significantly to this interaction. Additionally, TPX2 does not require the tubulin E-hook for microtubule binding, suggesting that other tubulin residues are responsible for the interaction.

Functional Eg5 from mammalian cell extracts

We prepared cytoplasmic extracts (19) from a mammalian cell line stably expressing full length, localization and affinity purification-tagged Eg5 (hereafter Eg5-EGFP) expressed from a bacterial artificial chromosome under control of the native promoter (12,20) (see Methods). The concentration of Eg5-EGFP in the cell extracts was determined using Western blotting; values of 20-60 nM were obtained depending on the extract (Fig. 3A). The concentration of TPX2 in these cytoplasmic extracts was less than ~1 nM, consistent with the localization of TPX2 to the nucleus during interphase (data not shown).

To analyze Eg5-EGFP motors in cell extracts, the extract was diluted into motility buffer (Methods) to achieve a final motor concentration of ~ 1 nM. Diluted extract was added to flow chambers containing rhodamine-labeled, taxol-stabilized microtubules immobilized to the surface using anti-tubulin antibodies (Methods). Using TIRF microscopy, bright puncta were observed to bind to the microtubules in the absence of ATP. Upon addition of ATP, robust motility of nearly all puncta was observed (Fig. 3B, Supplemental Movie 1). We observed an accumulation of motors at one end of most microtubules in the field of view (Fig. 3B; Supplemental Movie 1) indicating that motors remain associated with the microtubule plus-end after motion. This is consistent with the previously observed tethering of microtubules near the microtubule end in sliding assays using *Xenopus* Eg5 (see below) (21). At higher motor concentration, microtubules were uniformly coated with fluorescence, and individual puncta could not be resolved. The average velocity of individual puncta was 14.7 ± 0.9 nm/s, (SEM, N = 205) similar to the velocity of purified *Xenopus* and *Drosophila* Eg5 motors (22-24) (Fig. 3D). The average association time of Eg5 with the microtubules was not determined because motors rarely dissociated over the course of a 10 min movie and longer movies resulted in photobleaching of individual puncta (Supplemental Movie 2). Finally, motor behavior was not altered following storage in liquid nitrogen for several

weeks, so a single extract could be used for multiple experiments, making this a robust and versatile method for studying motor behavior (see Discussion).

To determine the directionality of motor motion, Kinesin-1-EGFP, a plus-end directed motor, was added to the chamber and the direction of motion observed. Next, the chamber was washed with 5 chamber volumes of ATP containing motility buffer, to remove the Kinesin-1-EGFP, and Eg5-EGFP was added to the same chamber and motor behavior was followed in the same field of view. In all cases, both Kinesin-1-EGFP and Eg5-EGFP moved to the same end of the microtubule (Fig. 3C) demonstrating that the motile puncta in the mammalian extract walk to the microtubule plus-end.

Next, we wished to determine if the Eg5-EGFP motors in the extract were present as tetramers. Because the cells expressing Eg5-EGFP also express endogenous Eg5, the motile motors could be composed of between 1 and 4 EGFP molecules. In this cell line, the Eg5-EGFP is not resistant to the siRNA designed to deplete endogenous Eg5 (12). Therefore, to estimate the number of labeled Eg5 motors in the motile puncta, we depleted endogenous Eg5 from parental cells co-transfected with siRNA resistant Eg5-mEmerald, and prepared cell extracts. The average fluorescence intensity of Eg5-mEmerald puncta was measured and compared with the fluorescence intensity of bacterially expressed Kinesin-1-EGFP dimers imaged under identical conditions (Fig. 3E). On average, the Eg5-mEmerald puncta were twice as bright as the Kinesin-1-EGFP dimers indicating that Eg5 was predominately tetrameric. The increase in quantum fluorescence yield of mEmerald alone is not sufficient to explain the nearly two-fold increase in fluorescence intensity (25). Additionally, the siRNA may not deplete 100% of the endogenous Eg5, which could form tetramers with the Eg5-mEmerald, resulting in decreased fluorescence of some puncta.

To determine if the Eg5-EGFP molecules function as tetramers, we examined the ability of Eg5-EGFP from extracts to crosslink two microtubules. To do this we added Eg5-EGFP to immobilized microtubules in a flow chamber and then added additional microtubules. The added microtubules bound to the immobilized microtubules and were translocated upon addition of ATP demonstrating that Eg5-EGFP was capable of crosslinking and sliding microtubules (Fig. 3F). In addition, the moving microtubule remained associated with the tip of the track microtubule, consistent with previous observations (21). Together, these experiments demonstrate that Eg5-EGFP from extracts is tetrameric (Fig. 3 E,F).

Next, we performed size exclusion chromatography on the extracts from LLC-Pk1 cells. Owing to the low abundance of

Eg5-EGFP in our extracts, we used cells overexpressing Eg5-mEmerald to aid in the detection. The western blots of the fractions obtained show that Eg5-mEmerald elutes around the same fractions as the Eg5-EGFP molecules, which are purified from SF9 insect cells, suggesting that the Eg5 molecules obtained from cell extracts are tetramers (Fig. 3G)

To demonstrate that the bright motile puncta derived from the cell extract are Eg5 molecules, we added S-trityl-L-cysteine (STLC) or 2-[1-(4-fluorophenyl)cyclopropyl]-4-(pyridin-4-yl)thiazole (FCPT) which specifically inhibit Eg5 (26,27). Each inhibitor completely stopped the motion of motile puncta (Fig. 3H); in the presence of FCPT, motors remained bound to the microtubule lattice, whereas in the presence of STLC, motors stopped walking and in many cases were released from the microtubule (22)(Fig. 3H).

Eg5 has been shown to exhibit diffusive behavior on microtubules at physiological salt concentration (22,28). To determine if mammalian Eg5 present in diluted cell extracts showed similar diffusive behavior, we added increasing concentrations of KCl to the motility buffer, and examined motor behavior. At 20 mM KCl, the velocity of Eg5 was 12.1 nm/s, similar to that observed in 0 mM KCl, and the diffusion coefficient, D, obtained from plots of MSD over time, was 1588 nm^2/s. At 50 mM KCl, motor velocity dropped to 3 nm/s and the value of D was 4556 nm^2/s (Fig. 3I). These results demonstrate that motor processivity is dependent on the ionic conditions, consistent with previous results using *Xenopus* Eg5 (23,28).

Together, our results show that Eg5-EGFP motors in mammalian cell extracts behave in a manner similar to purified *Xenopus* and *Drosophila* Eg5 tetramers. Specifically, the velocity, directionality, sensitivity to STLC and FCPT and diffusive behavior in higher ionic strength buffer are all consistent with previously reported properties of purified *Xenopus* and *Drosophila* Kinesin-5 motors. Somewhat surprisingly, the behavior of mammalian Eg5 motors has not been previously examined. Our data show that these motors are similar to insect and other vertebrate Eg5 motors and distinct from kinesin-5 motors from yeast that show directional switching (29,30). Importantly, the similar properties of the mammalian motors strongly suggests that components that are present in the cell extract do not have a major effect on motor behavior.

Interactions of TPX2 with the microtubule and with Eg5 both contribute to inhibition of motility

Previous work demonstrated that the gliding of microtubules by surface attached Eg5 dimers is inhibited by TPX2 full length

and to a lesser extent by TPX2-710 (11). Full length TPX2 also inhibits Eg5 mediated microtubule-microtubule sliding (11). In both of these assays, however, the behavior of populations of motors is examined, so how individual Eg5 molecules are regulated by TPX2 was not revealed. To gain a better understanding of the mechanism of inhibition of Eg5 by TPX2, we performed single molecule experiments.

To determine the effect of TPX2 on Eg5 behavior, the cytoplasmic extract containing Eg5-EGFP was diluted in motility buffer, added to chambers of immobilized microtubules, and motors were imaged. Next, TPX2 was added to the chamber during image acquisition (Fig. 4A). For these experiments, the velocity of motors following addition of TPX2 is expressed as a percentage of the velocity prior to addition of TPX2. The data show that full-length TPX2 is a potent inhibitor of the velocity of individual Eg5 motors: at 250 nM, TPX2 reduced Eg5 velocity by 83% and at 50 nM Eg5 velocity was reduced by 32% (Fig. 4B). To understand how the interaction of TPX2 with Eg5 contributes to motor inhibition, we repeated the experiment using TPX2-710. Addition of TPX2-710 also substantially reduced the velocity of Eg5-EGFP indicating that microtubule binding by TPX2 contributes to the reduction in motor velocity. At low concentrations (50 nM) both TPX2 and TPX2-710 showed similar inhibition of Eg5 (32% and 24% respectively. However, at higher concentrations (250 nM) TPX2-710 was a less effective inhibitor of Eg5-EGFP than TPX2 full length (inhibition of 53% and 83%, respectively) (Fig. 4B).

The results further show that TPX2 reduces the velocity of Eg5-EGFP motors without inducing dissociation of most motors from the microtubule (Fig. 4A) consistent with the established role of TPX2 in targeting Eg5 to spindle microtubules (11). In the presence of TPX2-710, more motors appeared to dissociate from the microtubule, although photobleaching precluded accurate quantification. In some cases, we saw that following addition of TPX2 to the motility chamber, motors from solution associated with the microtubule, and these motors also moved with reduced velocity (Fig. 4A).

To confirm the specificity of the Eg5-TPX2 interaction, we added full length TPX2-Halo covalently tagged with an Alexa 660 ligand to Kinesin-1-EGFP dimers in a single molecule assay (Fig. 4C). Consistent with prior results from microtubule gliding assays, TPX2 addition did not alter the motility of Kinesin-1-EGFP (11).

To visualize the interaction between Eg5 and TPX2 in the single molecule experiments, we used TPX2-Halo covalently tagged with an Alexa 660 ligand (Fig. 4D). In this experiment, addition of TPX2-Halo (at 20 nM) reduced the velocity of Eg5-EGFP. Analysis of kymographs showed that

individual motors that encountered TPX2-Halo walked at reduced velocity. In some cases a motor that has reduced velocity can resume motion when it encounters an area of the microtubule that is relatively free of TPX2 (Fig. 4D, right panels; Supplemental Movie 3). Note that in this experiment, a lower concentration of TPX2 was used because at higher concentration, fluorescent TPX2 coated the entire microtubule surface.

We also performed experiments in which 50 nM TPX2 or TPX2-710 was pre-mixed with the motor in motility buffer before addition to the chamber. This method allows Eg5 and TPX2 to potentially interact, and both molecules are introduced to the chamber simultaneously (Fig. 4E,F). This experiment also showed greater inhibition of Eg5-EGFP by the full-length compared to the truncated TPX2 (Fig. 4E,F). Interestingly, pre-mixing full-length TPX2 with Eg5-EGFP resulted in greater inhibition than when the same concentration of TPX2 was added to motors pre-bound to microtubules (60% vs. 32% inhibition, Fig. 4B, F). This result indicates that when the motor and TPX2 bind to the microtubule at the same time, stronger inhibition results. In contrast, when TPX2 is added to motors already bound to microtubules, TPX2 can bind to the microtubule at sites distant from the motors, and thus not immediately impact motor velocity. Interestingly, in the case of TPX2-710, inhibition of Eg5-EGFP was similar regardless of whether the motors were premixed or added sequentially (Fig. 4B, F).

Finally, to exclude the possibility that adding a Halo tag to TPX2 affected the TPX2-Eg5 interaction, we compared inhibition of Eg5 by untagged and Halo tagged TPX2. As seen in Fig. 4F, inhibition of Eg5-EGFP by TPX2 was not changed by the presence of the Halo tag demonstrating that the Halo tag was not detectably affecting TPX2-Eg5 interaction (Fig. 4F).

Together, the results of these experiments demonstrate that Eg5 in cytoplasmic extracts is inhibited by TPX2. Full length TPX2, which can interact with Eg5 and with the microtubule, is a more potent inhibitor than TPX2-710, which lacks the Eg5 interaction domain. However, by binding to the microtubule lattice, TPX2-710 also substantially reduces the velocity of individual Eg5 puncta.

TPX2 differentially inhibits Microtubule gliding by Eg5 dimers, but not monomers

To determine how Eg5-EGFP motors are inhibited by TPX2, we performed microtubule gliding assays using Eg5 dimers and Eg5 monomers (Methods). Dimers supported microtubule gliding at an average rate of ~20 nm/s. The velocity of gliding was reduced to ~6 nm/s by 250 nM full length TPX2; addition of the same concentration of TPX2-710 reduced the velocity of gliding to

~15 nm/s, demonstrating that TPX2-710 was a less effective inhibitor than the full length protein (Fig. 5A). This result demonstrates that dimeric Eg5 retains the ability to interact with TPX2, consistent with previous *in vitro* binding assays (11). In contrast, the velocity of microtubule gliding driven by monomeric Eg5 was inhibited to a similar extent by either full length or truncated TPX2 (Fig. 5B). It should be noted that the velocity of microtubule gliding driven by monomeric Eg5 is approximately half the rate of the dimeric construct, presumably due to the uncoordinated action of monomers. Further, our results also show that monomer-driven microtubule gliding is inhibited at lower concentrations of TPX2 or TPX2-710 (Fig. 5B). For example, addition of 25 nM TPX2 or TPX2-710 nearly completely halted microtubule gliding by monomeric Eg5 whereas a 20-fold greater concentration of TPX2 is required to result in a similar reduction in the velocity of microtubule gliding by Eg5 dimers. The reason for this increased sensitivity is not known, but may relate to the presence of a single motor head. These results suggest that the stalk region in the dimeric construct, or the dimer conformation, is required for differential inhibition by TPX2 and TPX2-710.

Discussion

TPX2 binding to microtubules

The results of our experiments provide insight into the interaction of TPX2 with the microtubule lattice. Our data show that TPX2 and TPX2-710 bind with relatively high apparent affinity to microtubules; these results are similar to the previously reported K_D of 0.5 μM for full length *Xenopus* TPX2 (31). The similar binding of TPX2 and TPX2-710 suggests that the C-terminal region is not a major contributor to microtubule binding, and instead interacts with the motor. The apparent affinity of TPX2 for microtubules is similar to other MAPs, including the dynein regulator, She1, MAP2 and Cep170 (15,32,33). The relatively strong interaction of TPX2 with the microtubule lattice is also reflected in the long dwell time measured for individual TPX2 puncta using microscopy (~60 s). Our experiments did not reveal a diffusive component to TPX2 behavior under the conditions used. Under physiological ionic conditions, however, we expect that TPX2 would bind less strongly to the microtubule lattice and could exhibit 1-D diffusive behavior that is characteristic of many MAPs.

Somewhat surprisingly, our results show that the C-terminal tails of tubulin, the E-hooks, do not contribute to TPX2 interaction with the microtubule. Other MAPs, including Tau, She1, and XMAP215 require the tubulin E-hooks for microtubule binding (15,34,35). Additionally, the processivity of Kinesin-1 and dynein motors, and the diffusive end targeting of MCAK, are enhanced by the E-hooks (36-

38). The observation that the interaction of TPX2 with microtubules does not require the E-hooks indicates that TPX2 binds to tubulin residues that are located between protofilaments, as opposed to along the ridge where the E-hooks are located. This is consistent with the observation that TPX2 does not inhibit single molecule motion of Kinesin-1-EGFP dimers on microtubules (Fig. 4C) and previous work demonstrating that TPX2 does not inhibit Kinesin-1 in a gliding assay (11). In contrast, Tau, which binds along the outer ridge and requires the E-hook for lattice diffusion (35), induces the release of kinesin motors, including both Kinesin-1 and Eg5, from the microtubule. This suggests that the location of MAP binding to the microtubule lattice results in differential effects on motor behavior (e.g. inhibition of motility vs. release) (11).

The high affinity interaction of TPX2 with microtubules is consistent with its established role in promoting microtubule assembly near kinetochores (8) and branched microtubules in the spindle (39). However, the interaction of TPX2 with microtubules in cells is dynamic, as evidenced by its poleward motion in the spindle (9). One possibility that can account for these differences is that modifications, such as phosphorylation, or interactions with other binding partners, such as dynein, regulate TPX2 dynamic behavior in cells.

Functional Eg5 from mammalian cell extracts

Previous work showed that the behavior of motors present in extracts of cultured mammalian or budding yeast cells is comparable to the behavior of the purified motor (13,30). We found that the rate of Eg5-EGFP stepping along the microtubule was ~14 nm/s in the plus-end direction, which is similar to the values obtained for purified *Xenopus* or *Drosophila* Eg5. To our knowledge, our results are the first report of single molecule data on the behavior of Eg5-EGFP tetramers from a mammalian source, although the behavior of human Eg5 dimers has been previously measured (40). Mammalian Eg5-EGFP showed exclusively plus-end directed motion at low salt and diffusive behavior at higher salt concentrations. At the highest salt concentration that we examined, no processive minus-end directed motion was detected, indicating that mammalian Eg5 does not show directional switching like the yeast homolog, Cin8 (29,30).

There are several potential advantages to using motors present in mammalian extracts for biophysical experiments. For example, the contribution of specific domains or potential phosphorylation sites can be determined using extracts prepared from cells transfected with fluorescent constructs encoding mutant versions of the protein of interest. Similarly, to eliminate binding partners, or accessory subunits implicated in

motor regulation or function, cells can be treated with siRNA prior to preparation of the extract. In addition, cells can be arrested at particular stages of the cell cycle prior to preparation of the extract to determine how cell cycle-dependent modifications may impact motor function. Finally, the ease of preparation and robust motile behavior demonstrate that biophysical measurements of motors from cell extracts is a powerful tool for future experiments.

TPX2 inhibits Eg5 by interactions with both the motor and microtubule

The single molecule data presented here demonstrate that TPX2 has two modes of inhibition for Eg5. Truncated TPX2 that cannot interact directly with Eg5, still bound to the microtubule lattice and substantially reduced the velocity of Eg5. Full-length TPX2, which binds to both the microtubule and the motor, was an even more potent inhibitor of Eg5. These results show that both binding to the microtubule and to Eg5 contribute to inhibition of the motor.

Our work is consistent with previous work demonstrating that MAPs can regulate motor behavior. For example, Tau results in differential regulation of Kinesin-1 and dynein; upon encountering a Tau patch, Kinesin-1 motors frequently detach from the microtubule, whereas dynein motors are likely to reverse direction or pause (41). However, a direct interaction of either Kinesin-1 or dynein with Tau has not been reported. Other MAPs function to target motors to microtubules. For example, Cep170, is important for targeting the kinesin-13, Kif2b, to the spindle (33) and the yeast microtubule associated protein She-1 prolongs the attachment of dynein to the microtubule in a stalled state in addition to inhibiting dynein motility (15). In contrast, the MAP ensconsin recruits and activates Kinesin-1 (42) independent of microtubule binding by ensconsin (43).

Recent *in vitro* experiments show that TPX2 inhibits the stepping behavior of the kinesin-12, Kif15, the human homolog of Xklp2 (44). TPX2 enhances the binding of Kif15 to microtubules in pelleting assays and increases motor binding to the microtubule under load in optical trapping experiments (44). Purified Eg5 has been shown to detach from the microtubule before stalling (45), suggesting that TPX2 may function to increase Eg5 binding to the microtubule under load, as is the case for Kif15. In mitotic cells, Eg5 and Kif15 act redundantly to establish and maintain spindle bipolarity. Furthermore, minus-end directed forces generated by cytoplasmic dynein antagonize force generated by these plus-end directed motors. Though TPX2 slows Eg5 and Kif15 motion on microtubules, by increasing the force generating capacity of these motors, it may play a key role in regulating forces needed for

spindle bipolarity.

Model for Regulation of Eg5 by TPX2

The data presented here are consistent with the following model for the regulation of Eg5 by TPX2 (Fig. 5C): Eg5 motors step along the microtubule protofilament and encounter TPX2, resulting in reduced velocity without inducing motor detachment from the microtubule. Our data showing that TPX2 does not require the E-hooks for microtubule binding suggest that TPX2 and Eg5 do not compete with each other for microtubule binding. The differential slowing of the motor by full length and truncated TPX2 demonstrates that binding of TPX2-710 to the microtubule is sufficient to reduce motor velocity but that the C-terminus of TPX2, which interacts with Eg5, results in stronger inhibition (Fig. 5C). This suggests that TPX2-710 acts as a slowing agent, reducing velocity when encountered by Eg5 motors. Additionally, our data suggest that the C-terminal domain may contribute to the retention of the motor on the microtubule (11). Although our experiments, and those of others (44), clearly demonstrate that TPX2 greatly reduces motor stepping on the microtubule, the TPX2-motor interaction must be regulated in live cells so that the motor can generate sliding forces to establish and maintain spindle bipolarity. Discovering precisely how this MAP-motor interaction is regulated spatially and temporally will provide important insight into spindle function *in vivo*.

Acknowledgements:

The authors would like to thank Mike Kimble and Aishwarya Vishwanath for assistance with single molecule tracking and Dr. Michael Gramlich for assistance with TIRF microscopy. We thank Dr. Sarah E Rice, Dr. Susan Gilbert and Dr. Michael Davidson for providing us with various Eg5 constructs. We thank Dr. W.-L. Lee for the Upl1 protease and we thank members of the Lee and Maresca labs for helpful comments on this work. JLR was supported by grant number NSF-DMR#1207783. The multi-color TIRF microscopy was performed on a user-supported instrument funded by a Major Research Instrumentation grant to JLR and PW NSF-DBI#0923318.

Conflict of interest. The authors declare that they have no conflicts of interest with the contents of this article.

Author contributions. PW and JLR designed the study. SKB performed the microtubule gliding and microtubule-microtubule sliding assays, and MSD experiments. SKB and BJM performed and analyzed the single molecule experiments. BJM cloned the Halo tagged constructs and performed the experiments in Figure 2. JT cloned the constructs expressed in Sf9 cells and performed preliminary experiments. PW wrote the paper. JLR graphed the data in Figure 3C. All authors analyzed the results, contributed to figure preparation and approved the final version of the manuscript.

References

1. Walczak, C. E., and Heald, R. (2008) Mechanisms of mitotic spindle assembly and function. *Int. Rev. Cytol.* **265**, 111-158
2. Wittmann, T., Boleti, H., Antony, C., Karsenti, E., and Vernos, I. (1998) Localization of the kinesin-like protein Xklp2 to spindle poles requires a leucine zipper, a microtubule-associated protein and dynein. *J. Cell Biol.* **143**, 673-685
3. Gruss, O. J., Wittmann, M., Yokoyama, H., Pepperkok, R., Kufer, T., Sillje, H., Karsenti, E., Mattaj, I. W., and Vernos, I. (2002) Chromosome-induced microtubule assembly mediated by TPX2 is required for spindle formation in HeLa cells. *Nat. Cell Biol.* **4**, 871-879
4. Garrett, S., Auer, K., Compton, D. A., and Kapoor, T. (2002) hTPX2 is required for normal spindle morphology and centrosome integrity during vertebrate cell division. *Curr. Biol.* **12**, 2055-2059
5. Kufer, T. A., Sillje, H. H. W., Korner, R., Gruss, O. J., Meraldi, P., and Nigg, E. A. (2002) Human TPX2 is required for targeting Aurora-A kinase to the spindle. *J. Cell Bio.* **158**, 617-623
6. Bayliss, R., Sardon, T., Vernos, I., and Conti, E. (2003) Structural basis of Aurora A activation by TPX2 at the mitotic spindle. *Mol. Cell* **12**, 851-862
7. Eyers, P. A., and Maller, J. L. (2004) Regulation of Xenopus Aurora A activation by TPX2. *J. Biol. Chem.* **279**, 9008-9015
8. Tulu, U. S., Fagerstrom, C., Ferenz, N. P., and Wadsworth, P. (2006) Molecular requirements for kinetochore-associated microtubule formation in mammalian cells. *Curr. Biol.* **16**, 536-541
9. Ma, N., Tulu, S., Ferenz, N., Fagerstrom, C., Wilde, A., and Wadsworth, P. (2010) Poleward Transport of TPX2 in mammalian spindles requires Eg5, dynein and microtubule flux. *Mol. Bio. Cell* **21**, 979-988
10. Eckerdt, F., Eyers, P. A., Lewellyn, A. L., Prigent, C., and Maller, J. L. (2008) Spindle pole regulation by a discrete Eg5-interacting domain in TPX2. *Curr. Biol.* **18**, 519-525

11. Ma, N., Titus, J., Gable, A., Ross, J. L., and Wadsworth, P. (2011) TPX2 regulates the localization and activity of Eg5 in the mammalian mitotic spindle. *J. Cell Biol.* **195**, 87-98
12. Gable, A., Qiu, M., Titus, J., Balchand, S., Ferenz, N. P., Ma, N., Fagerstrom, C., Ross, J. L., Yang, G., and Wadsworth, P. (2012) Dynamic reorganization of Eg5 in the mammalian spindle throughout mitosis requires dynein and TPX2. *Mol. Biol. Cell* **23**, 1254-1266
13. Cai, D., Verhey, K. J., and Meyhofer, E. (2007) Tracking single kinesin molecules in the cytoplasm of mammalian cells. *Biophys J* **92**, 4137-4144
14. Lowry, O. H., Rosenbrough, N. J., Farr, A. L., and Randall, R. J. (1951) Protein measurement with the Folin phenol reagent. *J. Biol. Chem.* **193**, 265-275
15. Markus, S. M., Kalutkiewicz, K. A., and Lee, W.-L. (2012) She1-mediated inhibition of dynein motility along astral microtubules promotes polarized spindle movements. *Curr Biol* **22**, 1-10
16. Larson, A. G., Naber, N., Cooke, R., Pate, E., and Rice, S. E. (2010) The conserved L5 loop establishes the pre-powerstroke conformation of the kinesin-5 motor, Eg5. *Biophys J* **98**, 2619-2627
17. Hyman, A., Drechsel, D., Kellogg, D., Salser, S., Sawin, K., Wordeman, L., and Mitchison, T. (1991) Preparation of modified tubulins. *Meth. Enzymol.* **196**, 478-485
18. Paschal, B. M., Obar, R. A., and Vallee, R. B. (1989) Interaction of brain cytoplasmic dynein and MAP2 with a common sequence at the C terminus of tubulin. *Nature* **342**, 569-572
19. Cai, D., McEwen, D. P., Martens, J. R., Meyhofer, E., and Verhey, K. J. (2009) Single molecule imaging reveals differences in microtubule track selection between kinesin motors. *PLOS Bio* **7**, e1000216
20. Cheeseman, I. M., and Desai, A. (2005) A combined approach for the localization and tandem affinity purification of protein complexes from metazoans. *Sci. STKE*, p11
21. Kapitein, L. C., Peterman, E. J. G., Kwok, B. H., Kim, J. H., Kapoor, T. M., and Schmidt, C. F. (2005) The bipolar mitotic kinesin Eg5 moves on both microtubles that it crosslinks. *Nature* **435**, 114-118
22. Kwok, B. H., Kapitein, L. C., Kim, J. H., Peterman, E. J. G., Schmidt, C. F., and Kapoor, T. M. (2006) Allosteric inhibition of kinesin-5 modulates its processive directional motility. *Nat. Chem. Biol.* **2**, 480-485
23. Kapitein, L. C., Kwok, B. H., Weinger, J. S., Schnmidt, C. F., Kapoor, T. M., and Peterman, E. J. G. (2008) Microtubule cross-linking triggers the directional motility of kinesin-5. *J. Cell Biol.* **182**, 421-428
24. van den Wildenberg, S. M. J. L., Tao, L., Kapitein, L. C., Schmidt, C. F., Scholey, J. M., and Peterman, E. J. G. (2008) The homotetrameric kinesin-5 KLP61F preferentially crosslinks microtubules into antiparallel orientations. *Curr. Biol.* **18**, 1860-1864
25. Day, R. N., and Davidson, M. W. (2009) The fluorescent protein palette: tools for cellular imaging. *Chem Soc Rev* **38**, 2887-2921
26. Groen, A. C., Needleman, D., Brangwynne, C., Gradinaru, C., Fowler, B., Mazitschek, R., and Mitchison, T. J. (2008) A novel small-molecule inhibitor

reveals a possible role of kinesin-5 in anastral spindle-pole assembly. *J. Cell Sci.* **121**, 2293-2300
27. Skoufias, D. A., DeBonis, S., Saoudi, Y., Lebeau, L., Crevel, I., Cross, R., Wade, R. H., Hackney, D., and Kozielski, F. (2006) S-trityl-L-cysteine is a reversible, tight binding inhibitor of the human kinesin Eg5 that specifically blocks mitotic progression. *J. Biol. Chem.* **281**, 17559-17569
28. Weinger, J. S., Qiu, M., Yang, G., and Kapoor, T. M. (2011) A nonmotor microtubule binding site in kinesin-5 is required for filament crosslinking and sliding. *Curr. Bio.* **21**, 154-160
29. Roostalu, J., Hentrich, C., Bieling, P., Telley, I. A., Schiebel, E., and Surrey, T. (2011) Directional switching of the kinesin Cin8 through motor coupling. *Science* **332**, 94-99
30. Gerson-Gurwitz, A., Thiede, C., Movshovich, N., Fridman, V., Podolskaya, M., Danieli, T., Lakamper, S., Klopfenstein, D. R., Schmidt, C. F., and Gherber, L. (2011) Directionality of individual kinesin-5 Cin8 motors is modulated by loop 8, ionic strength and microtubule geometry. *EMBO J.* **30**, 4942-4954
31. Wittmann, T., Wilm, M., Karsenti, E., and Vernos, I. (2000) TPX2, a novel Xenopus MAP involved in spindle pole organization. *J. Cell Biol.* **149**, 1405-1418
32. Illenberger, S., Drewes, G., Trinczek, B., Biernat, J., Meyer, H. E., Olmsted, J. B., Mandelkow, E.-M., and Mandelkow, E. (1996) Phosphorylation of microtubule-associated proteins MAP2 and MAP4 by the protein kinase p110mark. *J. Biol. Chem.* **271**, 10834-10843
33. Welburn, J. P. I., and Cheeseman, I. M. (2012) The microtubule-binding protein Cep170 promotes the targeting of the kinesin-13 depolymerase Kif2b to the mitotic spindle. *Mol Biol Cell* **23**, 4786-4796
34. Brouhard, G. J., Stear, J. H., Noetzel, T. L., Al-Bassam, J., Kinoshita, K., Harrison, S. C., Howard, J., and Hyman, A. A. (2008) XMAP215 is a processive microtubule polymerase. *Cell* **132**, 79-88
35. Hinrichs, M. H., Jalal, A., Brenner, B., Mandelkow, E., Kumar, S., and Scholz, T. (2012) Tau protein diffuses along the microtubule lattice. *J. Biol. Chem.* **287**, 38559-38568
36. Helenius, J., Brouhard, G. J., Kalaidzidis, Y., Diez, S., and Howard, J. (2006) The depolymerizing kinesin MCAK uses lattice diffusion to rapidly target microtubule ends. *Nature* **441**, 115-119
37. Thorn, K. S., Ubersax, J. A., and Vale, R. D. (2000) Engineering the processive run length of the kinesin motor. *J Cell Biol* **151**, 1093-1100
38. Wang, Z., and Sheetz, M. P. (2000) The C-terminus of tubulin increases cytoplasmic dynein and kinesin processivity. *Biophys. J.* **78**, 1955-1964
39. Petry, S., Groen, A. C., Ishihara, K., Mitchison, T. J., and Vale, R. D. (2013) Branching microtubule nucleation in Xenopus egg extracts mediated by augmin and TPX2. *Cell* **152**, 768-777
40. Valentine, M. T., Fordyce, P. M., Krzysiak, T. C., Gilbert, S. P., and Block, S. M. (2006) Individual dimers of the mitotic kinesin motor eg5 step processively and support substantial loads in vitro. *Nat. Cell Bio.* **8**, 470-476
41. Dixit, R., Ross, J. L., Goldman, Y. E., and Holzbaur, E. L. (2008) Differential regulation of dynein and kinesin motor proteins by Tau. *Science* **319**, 1086-1089

42. Sung, H.-H., Telley, I. A., Papadaki, P., Ephrussi, A., Surrey, T., and Rorth, P. (2008) Drosophila Ensconsin promotes productive recruitment of kinesin-1 to microtubules. *Devel. Cell* **15**, 866-876
43. Barlan, K., Lu, W., and Gelfand, V. I. (2013) The microtubule-binding protein ensconsin is an essential cofactor of kinesin-1. *Curr. Biol.* **23**, 317-322
44. Drechsler, H., McHugh, T., Singleton, M. R., Carter, N. J., and McAinsh, A. D. (2014) The kinesin-12 Kif15 is a processive track-switching tetramer. *eLIFE* **3**, e01724
45. Korneev, M. J., Lakamper, S., and Schmidt, C. F. (2007) Load-dependent release limits the processive stepping fo the tetrameric Eg5 motor. *Eur. Biophys. J.* **36**, 675-681

Figure Legends

Figure 1. Binding of TPX2 and TPX2-710 to microtubules. (A) Schematic diagram of the TPX2 constructs (left) and Commassie Brilliant Blue stained gel of the purified proteins (right). (B) Co-sedimentation of TPX2 with microtubules; S-supernatant; P-pellet. Concentration of microtubules in each pair of lanes is noted above. Western blots stained for TPX2 or tubulin. (C) Quantification of apparent affinity was performed using a quadratic fit. Experiment was performed twice and the values averaged; marker bars show standard deviation.

Figure 2. Binding Dynamics of TPX2 and TPX2-710 (A) Box plot showing release of TPX2 and TPX2-710 from microtubules in the presence of the indicated concentration of KCl added to the buffer. TPX2 fluorescence reported as AU = arbitrary units. Whiskers define the range, boxes encompass 25th to 75th quartiles, lines depict the medians. (B) TPX2 and TPX2-710 binding to untreated and Subtilisin A digested microtubules; (upper panels) fluorescence images of TPX2-Halo or TPX2-710-Halo bound to untreated and Subtilisin A digested microtubules; (middle) quantification of TPX2 fluorescence; (lower) polyacrylamide gel showing digested and control microtubules. TPX2 fluorescence measured for at least 60 microtubules for each of two independent experiments; error bars = SD. (C) Kymograph of TPX2-Halo and TPX2-710-Halo on microtubules. Vertical scale (time) is 60 s; horizontal scale bar is 2 μm.

Figure 3. Characterization of Eg5 in mammalian cell extracts. (A) Western blot of cell extract and purified Eg5. (B) Schematic diagram of the single molecule TIRF experiments (left) and TIRF images of Eg5-EGFP accumulating at the microtubule plus-end (right). (C) Kymographs of Eg5-EGFP and Kinesin-1 EGFP dimers on the same microtubule. Note the different time scale. Plus and minus ends of the microtubules are indicated. (D) Histogram of Eg5-EGFP motor velocity. (E) Histogram of the fluorescence of Kinesin-1 dimers (light gray) and Eg5 molecules (dark gray) in the extract. (F) Schematic diagram (left) and fluorescence images (right) showing microtubule-microtubule sliding by Eg5. Arrowhead marks the end of the sliding microtubule. (G) Coomassie Brilliant Blue stained gel of Eg5-EGFP purified from insect cells and the trace of absorbance at 488nm on the size exclusion column for the purified protein. The western Blot shown is for the fractions obtained from size exclusion chromatography of Eg5-mEmerald from LLC-Pk1 extract probed for Eg5. (H) Quantification of the velocity of Eg5-EGFP after addition of DMSO, STLC or FCPT (right). Error bars = SEM. (I) Directional and diffusive motility of Eg5-EGFP in the presence of 0, 20 or 50 mM KCl added to the motility buffer. Kymographs (upper) and mean squared displacement (lower). Horizontal scale bar in B, C, F, H is 1 μm; vertical scale bar in G, H is 60 s. Vertical scale in C is provided on the image.

Figure 4. Inhibition of Eg5 by TPX2 requires both binding to the microtubule and an interaction between TPX2 and Eg5. (A) Kymographs of Eg5-EGFP before and following addition of TPX2 or TPX2-710; arrowhead marks time of TPX2 addition. (B) Quantification of Eg5-EGFP velocity; error bars = SD. (C) Kymograph of Kinesin-1 EGFP dimers walking on microtubules before and after addition of TPX2 (arrowhead). 1 nM Kinesin-1 EGFP (green) and 500 nM TPX2-Halo (red) were used. (D) Kymographs of Eg5-EGFP (green) before and following addition of 20 nM TPX2-Halo (red). Right panels show enlarged view. (E) Kymographs of Eg5-EGFP that was pre-mixed with TPX2-Halo or TPX2-710-Halo. (F) Quantification of Eg5-EGFP velocity in the presence of 50 nM TPX2 that was Halo tagged (left) or untagged (right). Error bars = SEM. Horizontal scale bars in A, C, E are 1 μm; horizontal scale bar in D is 2 μm; vertical scale bar in A,D,E is 60 s and is 5 s in C.

Figure 5. Differential regulation of Eg5 dimers, but not monomers, by full length and truncated TPX2. Velocity of microtubule gliding driven by (A) Eg5 dimers or (B) Eg5 monomers. Error bars show SEM. (C). Model for inhibition of Eg5 by TPX2. Top shows inhibition of motor stepping by full length (left, stop symbol) and truncated TPX2 (right, slow

symbol) in single molecule assays. Lower panels show inhibition of microtubule gliding by Eg5 dimers (top) and Eg5 monomers (bottom). Eg5 - green; TPX2 - orange.

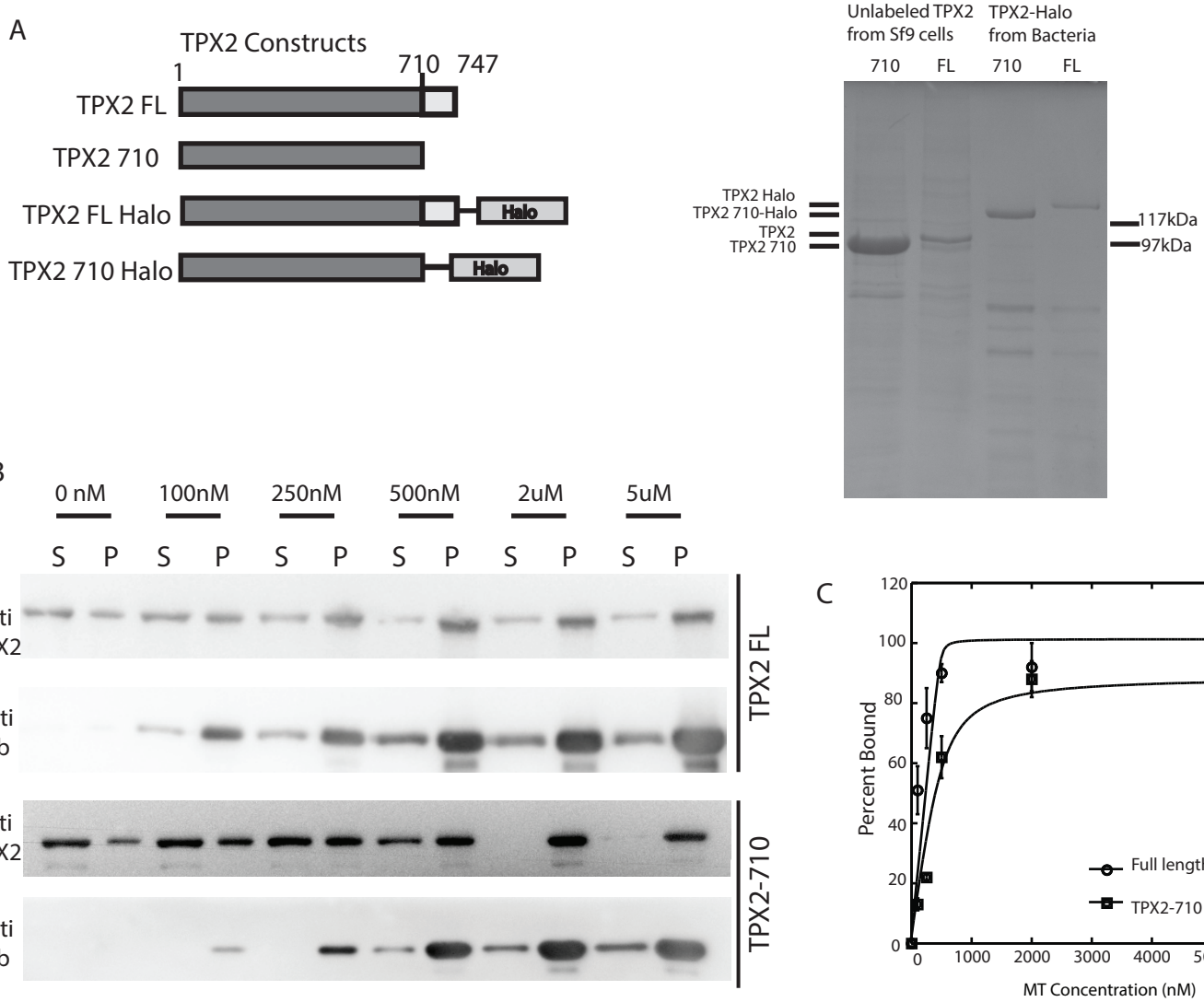

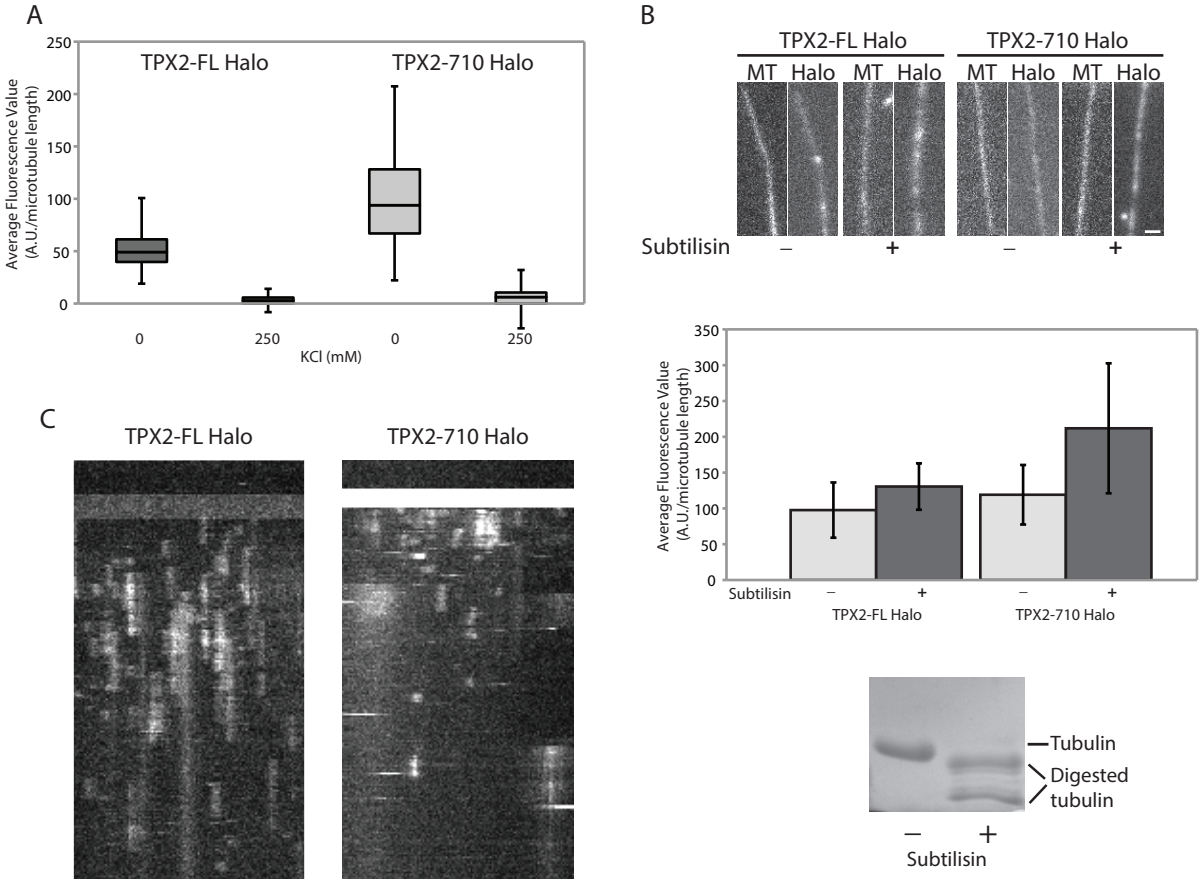
A
TPX2-FL Halo
TPX2-710 Halo
Average Fluorescence Value (A.U./microtubule length)
250
200
150
100
50
0
0
250
0
250
KCl (mM)
B
TPX2-FL Halo
TPX2-710 Halo
MT Halo MT Halo
MT Halo MT Halo
Subtilisin
–
+
–
+
Average Fluorescence Value (A.U./microtubule length)
350
300
250
200
150
100
50
0
Subtilisin
–
+
–
+
TPX2-FL Halo
TPX2-710 Halo
Tubulin
Digested tubulin
–
+
Subtilisin
C
TPX2-FL Halo
TPX2-710 Halo

Figure 3

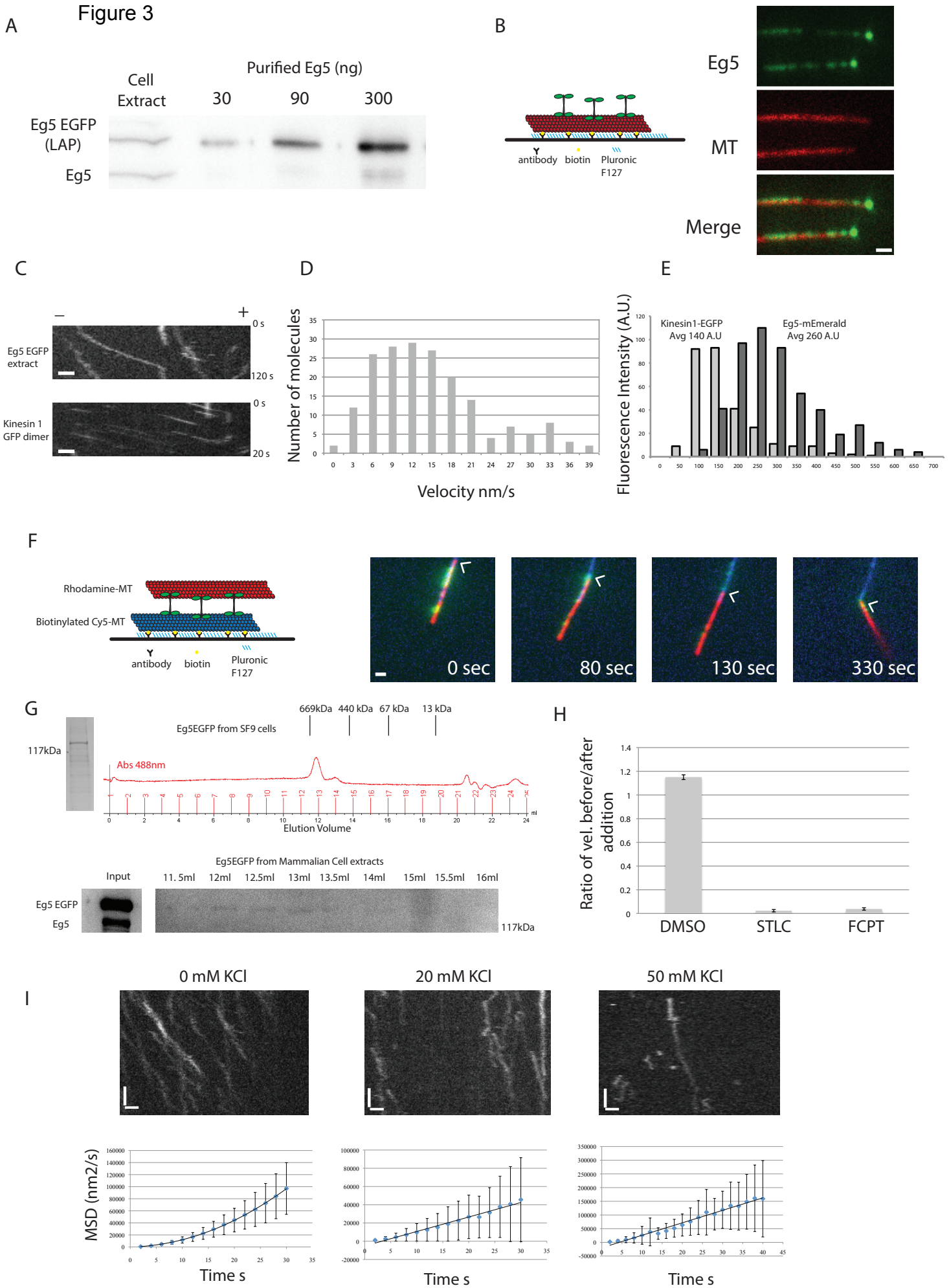
A
Cell Extract
Purified Eg5 (ng)
30
90
300
Eg5 EGFP (LAP)
Eg5
B
antibody
biotin
Pluronic F127
Eg5
MT
Merge
C
–
+
0 s
120 s
Eg5 EGFP extract
0 s
20 s
Kinesin 1 GFP dimer
D
Number of molecules
Velocity nm/s
E
Fluorescence Intensity (A.U.)
Kinesin1-EGFP Avg 140 A.U
Eg5-mEmerald Avg 260 A.U
F
Rhodamine-MT
Biotinylated Cy5-MT
antibody
biotin
Pluronic F127
0 sec
80 sec
130 sec
330 sec
G
117kDa
669kDa 440 kDa 67 kDa 13 kDa
Eg5EGFP from SF9 cells
Abs 488nm
Elution Volume
Eg5EGFP from Mammalian Cell extracts
Input
11. 5ml 12ml 12.5ml 13ml 13.5ml 14ml 15ml 15.5ml 16ml
Eg5 EGFP
Eg5
117kDa
H
Ratio of vel. before/after addition
DMSO
STLC
FCPT
I
0 mM KCl
20 mM KCl
50 mM KCl
MSD (nm2/s)
Time s
Time s
Time s

A

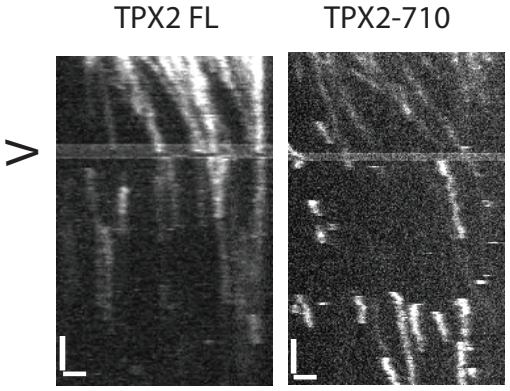

B

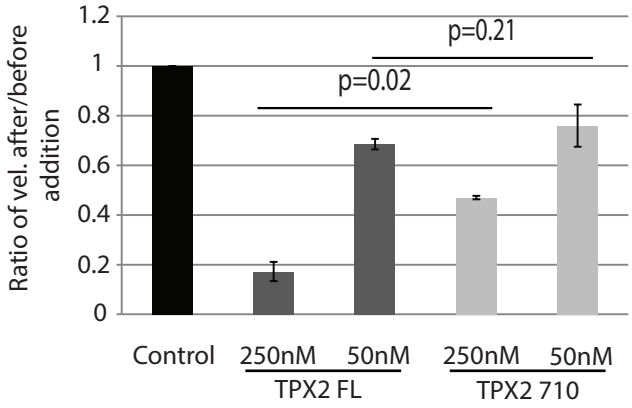

C

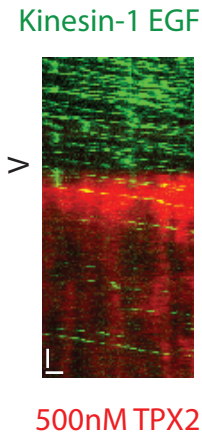

D

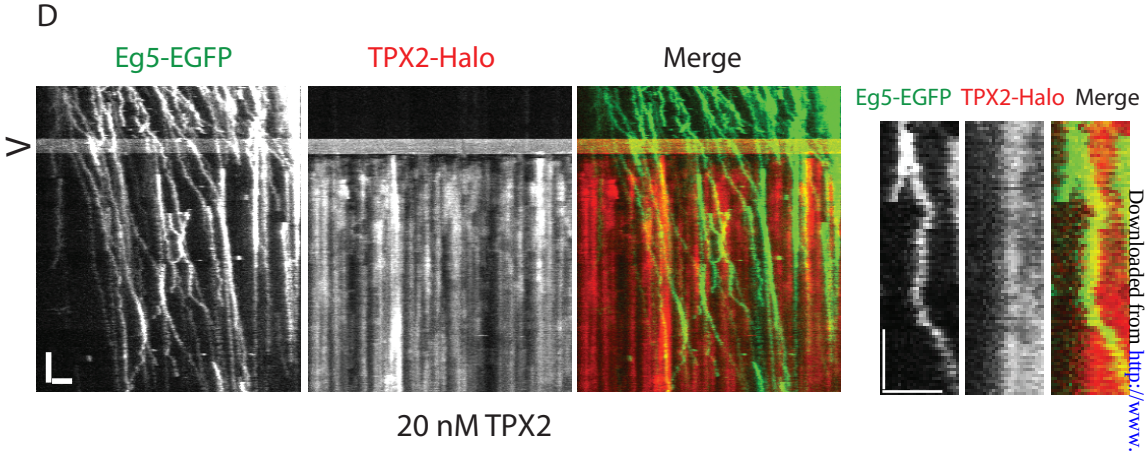

E

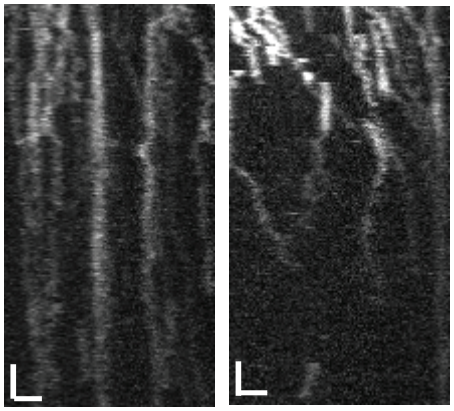

F

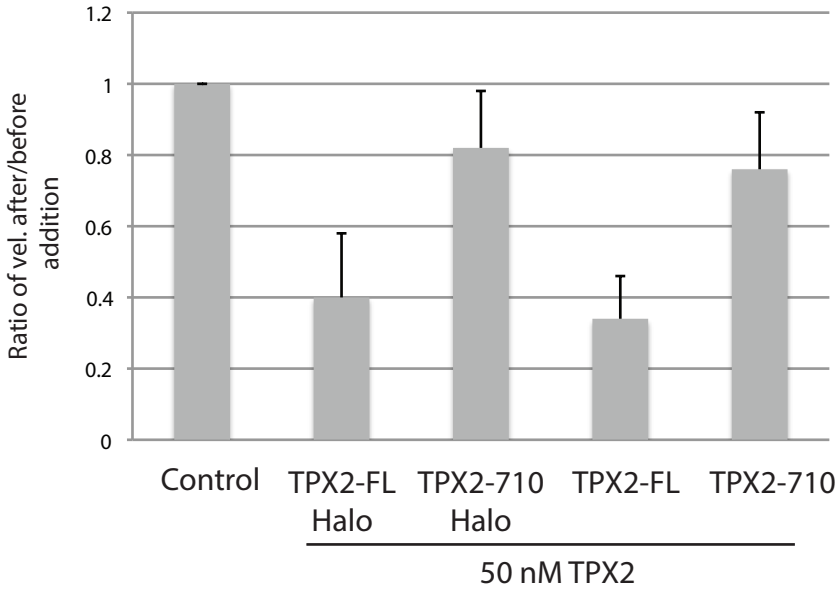

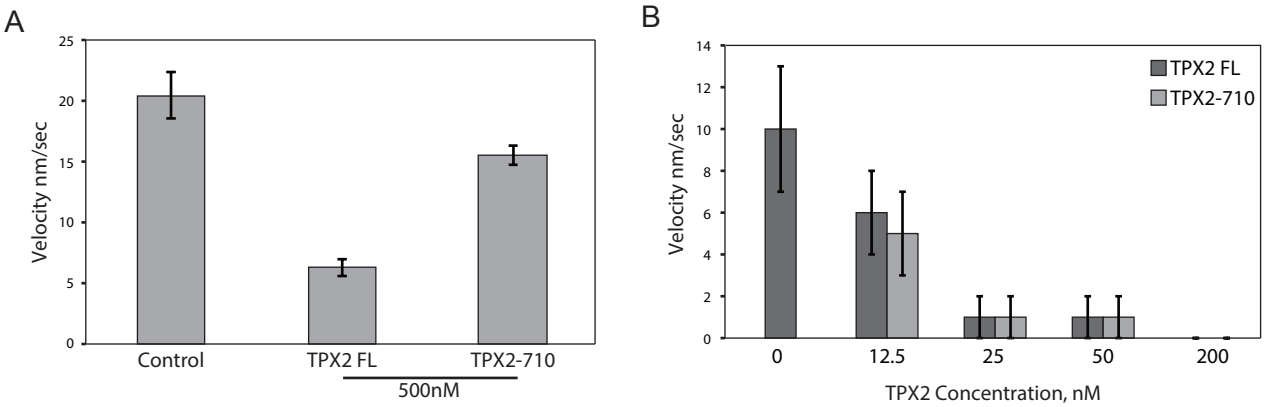
A
Velocity nm/sec
25
20
15
10
5
0
Control
TPX2 FL
TPX2-710
500nM
B
Velocity nm/sec
14
12
10
8
6
4
2
0
TPX2 FL
TPX2-710
0
12.5
25
50
200
TPX2 Concentration, nM

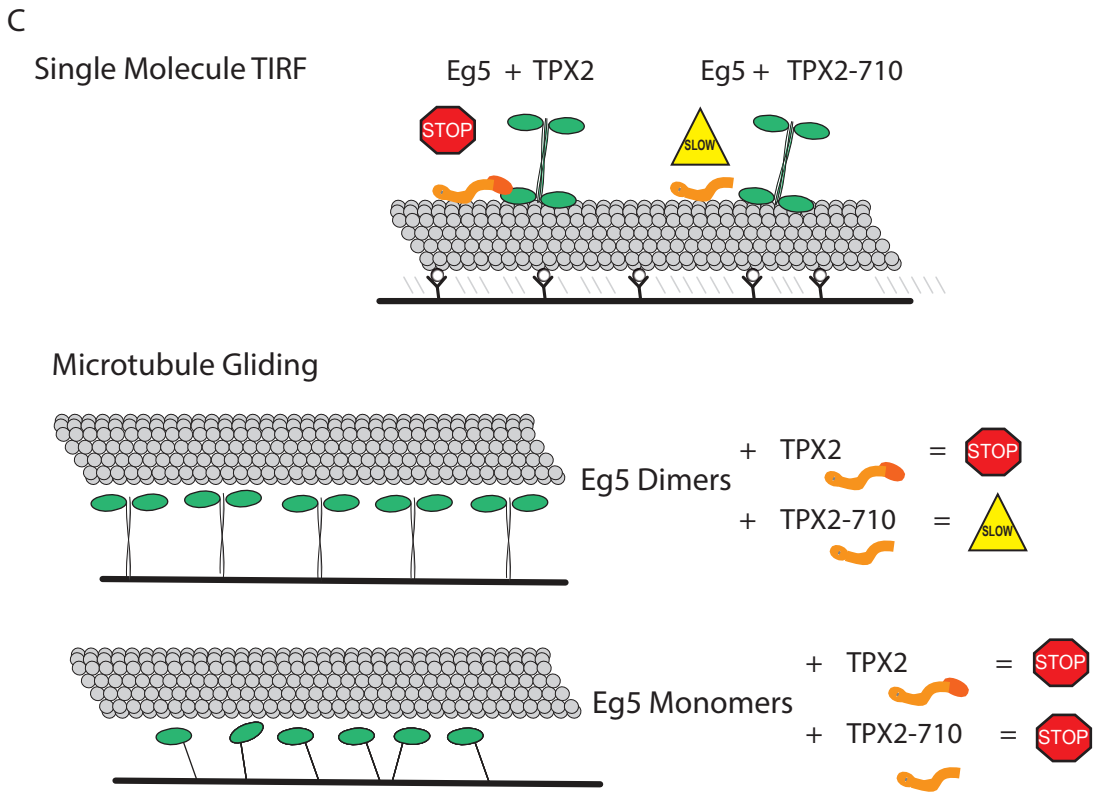
C
Single Molecule TIRF
Eg5 + TPX2
Eg5 + TPX2-710
STOP
SLOW
Microtubule Gliding
Eg5 Dimers
+ TPX2 = STOP
+ TPX2-710 = SLOW
Eg5 Monomers
+ TPX2 = STOP
+ TPX2-710 = STOP

Cell Biology:

TPX2 Inhibits Eg5 by Interactions with both Motor and Microtubule

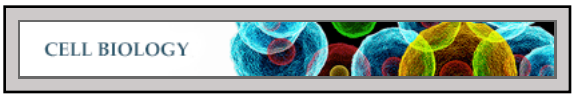

Sai K. Balchand, Barbara J. Mann, Janel Titus, Jennifer L. Ross and Patricia Wadsworth

J. Biol. Chem. *published online May 27, 2015*

Access the most updated version of this article at doi: 10.1074/jbc.M114.612903